Available online at www.sciencedirect.com

ScienceDirect

Journal of Nuclear Materials 362 (2007) 466–473

journal of nuclear materials

www.elsevier.com/locate/jnucmat

Solid state diffusion during nuclear glass residual alteration in solution

T. Chave [a,*], P. Frugier [a], A. Ayral [b], S. Gin [a]

[a] Commissariat à l'Énergie Atomique – CEA Valrhô DTCD/SECM/LCLT, BP 17171, 30207 Bagnols-sur-Cèze cedex, France
[b] Institut Européen des Membranes, UMR 5635, CNRS-ENSCM-UMII, CC047, Université Montpellier II,
F-34095 Montpellier cedex 5, France

Abstract

The long term alteration rate of the French R7T7 nuclear glass has been investigated since many years because this glass has been selected as radionuclide containment matrix in France. Recent studies have shown that this rate remains constant or is slightly decreasing with time. It never reaches zero. Although this long term rate is very low, only 5 nm per year at 323 K in initially pure water, it would be the dominant alteration phenomenon in a geological repository. Two mechanisms are suggested for explaining this long term behaviour: diffusion towards solution of elements from glass through an amorphous altered layer and precipitation of neoformed phases. Former studies showed that diffusion rates are in agreement with a solid state diffusion mechanism. Additional experiments in initially saturated silica water were performed in order to study the impact of various parameters on the values of the diffusion coefficient for mobile chemical elements: pH, temperature, ionic strength and S/V ratio (glass surface area S to the solution volume V). The solutions and element profiles in altered glass were analysed by ICP-AES and TOF-SIMS, respectively. The results point out that S/V and ionic strength are not key-parameters. pH leads to significant diffusion coefficient decrease at 323 K when it rises from 8 to 10. Variations with temperature can be modelled with an Arrhenius law. The calculated value of activation energy is discussed in comparison with literature data.

PACS: 28.41.Kw; 62.20.Mk

---

1. Introduction

Borosilicate glass has been chosen as containment matrix for French high level wastes (HLW) due to its strong chemical stability. Experimental data show that its long term alteration rate does not exceed tens of nanometres per year at 363 K [1]. In order to simulate conditions corresponding to the geological repository environment, the study of the long term glass leaching at 'short' laboratory time scale (a few years) requires specific conditions and tools, as described later.

In contact with water, glass network bonds are broken and exchange occurs between water or H^+ ions and glass components. This leaching is observed for mobile elements such as boron or alkalis. However, it is also true for glass formers: Si–O–B and Si–O–Si bonds are broken during the first steps of the alteration. At this point, alteration rate is maximal. It is about $1\ g\ m^{-2}\ d^{-1}$ at 363 K for

---

[*] Corresponding author. Tel.: +33 466797694; fax: +33 466796620.
E-mail address: tony.chave@cea.fr (T. Chave).

0022-3115/$ - see front matter © 2007 Elsevier B.V. All rights reserved.
doi:10.1016/j.jnucmat.2007.01.095

R7T7 glass in pure water [2]. Then the solution becomes 'saturated', i.e. the Si concentration reaches a limiting steady-state value. This saturation in silicon triggers a decrease in leaching rate by 3–4 orders of magnitude [3–5]. In the solid, at the same time, an amorphous protective layer named *gel*, is formed, resulting of the silicon recondensation in the former fresh glass in contact with water. This altered layer will change and may acquire protective properties with time [1,6–8]. After this kinetic drop, the glass is expected to enter in a steady alteration state called residual rate governed by two main mechanisms [9]: the solid state diffusion and the precipitation of neoformed phases such as phyllosilicates and zeolites [9–12]. Temperature, pH and S/V ratio (ratio of the glass surface area S to the volume of water in contact V) are key-parameters for the overall glass and gel behaviour.

Nevertheless theses parameters do not have the same impact on the different alteration states. This paper will focus on the effect of these parameters on the long term behaviour which will define the overall resistance of the containment matrix. Si pre-saturated solution and high S/V ratio are used in order to obtain conditions simulating the long term corrosion in a short experimental time. In fact, by using initially saturated silicon solution, transient alteration states are excluded and the formation of a protective and homogeneous layer from the start of the leaching reaction is allowed. This is a key parameter for studying the solid state diffusion in a proper way which is the aim of this paper [13]. On the other hand, the interest in high S/V ratio, is that the solution in contact is very rapidly enriched in mobile elements. Thus, solution concentrations, especially in Na, Li and B, can vary on several orders of magnitude during the leaching and may have an influence on diffusion phenomena. Therefore, several experiments with different background electrolyte concentrations are carried out in order to investigate this factor.

In the same way, as alteration layers do not exceed tens of nanometres, Time Of Flight-Secondary Ion Mass Spectrometry (TOS-SIMS) is the most suitable method to carry out relevant depth profile solid analyses.

2. Materials and methods

2.1. Experimental procedure

The glass studied in this work is the SON68 glass, which is an inactive glass whose composition is described in Table 1. All experiments are carried out in static system within 180 mL PTFE reactors. Amorphous silica is initially dissolved in the solution to obtain a 150 ppm Si concentration, which is above the saturated value of SON68 Glass at 363 K and pH 9. This concentration enables to be oversaturated with respect to chalcedony for all experimental conditions. A previous study showed that silicon concentration measured in solution is close to that of chalcedony [14]. The different experiments are listed in Table 2.

pHs were adjusted to and maintained at the indicated values through addition of sodium hydroxide one molar solution. Moreover, for two experiments, the ionic strength was fixed – by adding into the initial solution, lithium and sodium chloride in 1:1 mass ratio – at values exceeding one to two orders of magnitude the ionic strength reached for similar experiments without addition of background electrolyte. Concerning S/V, a 2 μm-sized powder with a specific area of 4.49 $m^2\,g^{-1}$ was used in order to obtain high S/V ratio, at 200 or 2000 cm^{-1}.

Solution aliquots were taken for all experiments at regular intervals over 2–4 months. These aliquots were ultrafiltrated with 10000 Dalton cells and acidified with 0.5 M HNO_3 prior to ICP-AES measurements.

Finally, TOF-SIMS depth profile analyses were carried out on glass pellets on TOF IV IONTOF device at Biophy research laboratory in Fuveau (France). All main glass components were analysed especially mobile elements in order to focus on solid state diffusion profiles.

2.2. Calculation methods

Element normalised mass losses are then calculated with solution analyses using the following equation:

Table 1
SON68 glass composition expressed in oxide weight percents

	SiO_2	B_2O_3	Al_2O_3	Na_2O	Li_2O	Cs_2O	CaO	Fe_2O_3	ZrO_2	ZnO	Nd_2O_3	La_2O_3	Pr_2O_3	Ce_2O_3	Others
Wt fraction (%)	45.5	14.0	4.9	9.9	2.0	1.1	4.0	2.9	2.7	2.5	1.6	0.9	0.5	1.0	6.5

Table 2
Overview of the experiment results

Experiment number	Time (d)	Temperature (K)	pH setting	Averaged pH over time	Initial S/V (cm^{-1})	Initial ionic strength (M)	D_B (m^2 s^{-1})	r^2 (–)
1	113	303 ± 1	9	8.95 ± 0.01	193 ± 1	<0.005	$(1.7 \pm 0.1) \times 10^{-24}$	0.9996
2	57	**303 ± 1**	10	9.82 ± 0.01	203 ± 1	<0.005	$(1.2 \pm 0.1) \times 10^{-24}$	0.9913
3	113	323 ± 1	**8**	8.15 ± 0.01	199 ± 1	<0.005	$(1.4 \pm 0.1) \times 10^{-23}$	0.9916
4	121	**323 ± 1**	**9**	9.00 ± 0.01	**202 ± 1**	**<0.005**	$(7.2 \pm 0.4) \times 10^{-24}$	0.9891
5	56	323 ± 1	9	9.04 ± 0.01	200 ± 1	**0.27 ± 0.01**	$(6.6 \pm 0.3) \times 10^{-24}$	0.9601
6	121	323 ± 1	**10**	9.95 ± 0.01	205 ± 1	<0.005	$(3.4 \pm 0.2) \times 10^{-24}$	0.9905
7	111	323 ± 1	9	9.02 ± 0.01	2026 ± 10	**0.27 ± 0.01**	$(2.6 \pm 0.2) \times 10^{-24}$	0.9957
8	58	323 ± 1	9	9.06 ± 0.01	**2020 ± 10**	**<0.005**	$(2.8 \pm 0.2) \times 10^{-24}$	0.9897
9	57	**363 ± 1**	8	8.20 ± 0.01	202 ± 1	<0.005	$(3.2 \pm 0.2) \times 10^{-22}$	0.9853
10	113	363 ± 1	9	9.04 ± 0.01	200 ± 1	<0.005	$(1.6 \pm 0.1) \times 10^{-22}$	0.9913

pH values are given at experiment temperatures. Amorphous silica is initially dissolved in all experiments in order to reach a 150 ppm Si concentration.

$$NL_i = \frac{C_i}{(S/V)X_i}, \tag{1}$$

where NL_i is the normalised mass loss in element i (g m^{-2}), S/V is the glass surface on solution volume ratio (m^{-1}), C_i is the concentration in element i (g m^{-3}) and X_i is the mass fraction of element i in the glass (–).

S/V ratio evolutions due to evaporation and aliquots are also taken into account. In the same way an alteration rate r_B (g m^{-2} d^{-1}) is defined, based on boron normalised mass loss as follows:

$$r_B = \frac{dNL_B}{dt}. \tag{2}$$

Altered glass thickness is assessed by dividing mobile element normalised mass loss by the glass density (2.75 g cm^{-3}). Boron is chosen for such calculation because this element is not retained in secondary phases and is one of the first diffusing glass components. Moreover, for all experiments solid apparent diffusion coefficients are determined by using Fick's second law and solution analyses. Hence, the gel thickness and its time dependency can be written as follows:

$$d_i = \frac{NL_i}{\rho_{glass}} = 2\sqrt{\frac{D_i \cdot t}{\pi}}, \tag{3}$$

where d_i is the equivalent gel thickness based on i element concentration (m^{-1}), ρ_{glass} is the glass density (g m^{-3}), D_i is the i element diffusion coefficient (m^2 s^{-1}) and t is the time (s).

Concerning the TOF-SIMS profiles, this paper will briefly discuss in what extend, solution based diffusion coefficients and TOF-SIMS based diffusion coefficients can be compared. For this purpose several assumptions are needed. The studied system is assumed to be an extended source, in a semi infinite media with a constant diffusion coefficient. According to Crank [15], the depth profiles have been modelled in the case of a simple one dimensional diffusion as

$$\frac{C}{C_0} = \operatorname{erf}\left(\frac{x}{2\sqrt{D \cdot t}}\right), \tag{4}$$

where x is the solid depth from the solution (nm) and erf is the *error function* defined as follows:

$$\operatorname{erf}(z) = \frac{2}{\sqrt{\pi}} \int_0^z \exp(-\eta^2)\, d\eta, \tag{5}$$

where η is a dummy variable.

3. Results

The results for all experiments are summarised in Table 2. Boron diffusion coefficients are given with the corresponding square root of time regression coefficients r^2. An example of gel thickness evolution versus time is pointed out in Fig. 1 with the square root of time fit in Fig. 2. Boron and other mobile elements have similar diffusion behaviour, since they are the first glass elements to be leached congruently with equivalent diffusion coefficients. Nevertheless, it has been observed that lithium diffuses in general slightly faster than sodium and boron. As pHs are not buffered, some variations are noticed and addition of molar sodium hydroxide or hydrochloric acid solutions is needed. Averaged pH values are given in Table 2.

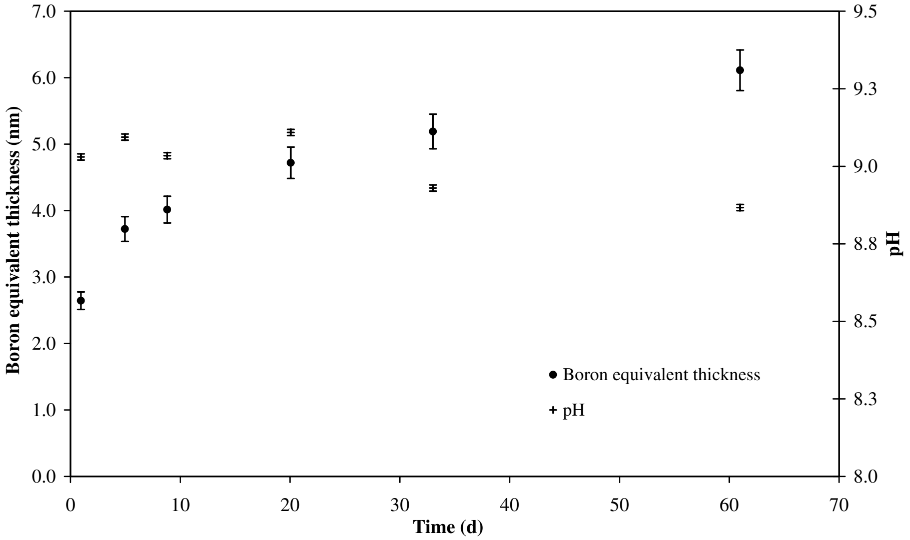

Fig. 1. Boron equivalent thickness and pH evolution versus time of the 303 K, 200 cm^{-1}, pH 9; 150 ppm Si experiment.

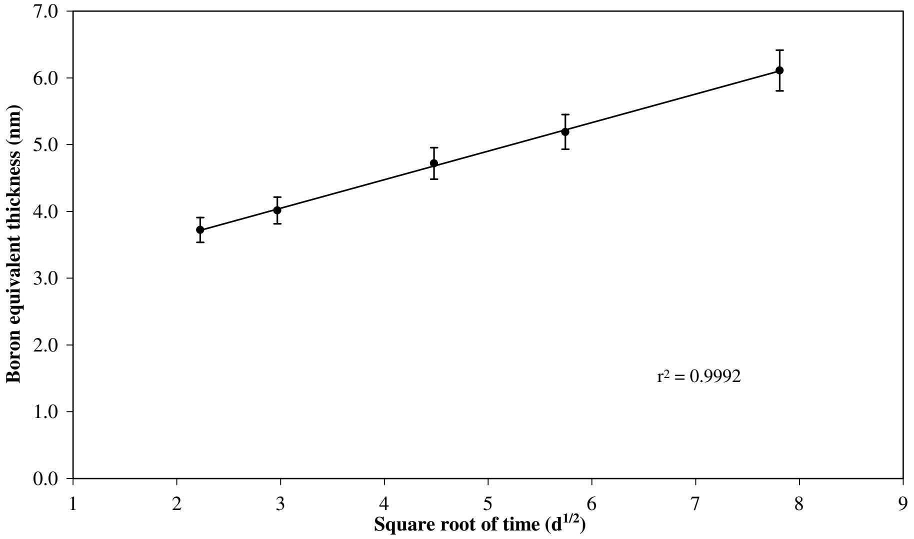

Fig. 2. Evolution of boron equivalent thickness versus square root of time. The experimental conditions are 303 K, 200 cm^{-1}, pH 9; 150 ppm Si.

As depicted in Figs. 1 or 2, it can be noticed that the d_B does not start from 0 but from about 3 nm. This can be explained by a very fast glass hydrolysis of surface sites. As a matter of fact, fine (1–2 μm sized) unwashed glass powder obtained by attrition, was used. Therefore, this early step hydrolysis is overstressed compared to usual 10–100 μm-sized powders. Monte Carlo and Ab-Initio numerical simulations are also in agreement with this experimental observation [16,17].

4. Discussion

4.1. Influence of ionic strength

According to ionic strength experiments, experiments number 4/5 and 7/8 in Table 2, it can be seen that the diffusion coefficients are very close when comparing both experiments at 200 cm^{-1} and at 2000 cm^{-1} and agree within the uncertainty range. It seems that ionic strength even at high values does not drastically influence diffusion phenomena during glass alteration.

4.2. Temperature and pH dependencies

In order to model the diffusion coefficients dependencies in pH and temperature, experimental values are separately plotted in Figs. 3 and 4. No specific experimental difficulties are encountered for pH study. However, for temperature dependency, pH is intrinsically related with temperature (variations of pK_w from 14 to 12.4 between 303 and 363 K). Since the experiments are carried out in basic solutions, the hydroxide ions are predominant. Thus, OH^- concentration poorly depends on temperature compared to H_3O^+ concentration. For modelling

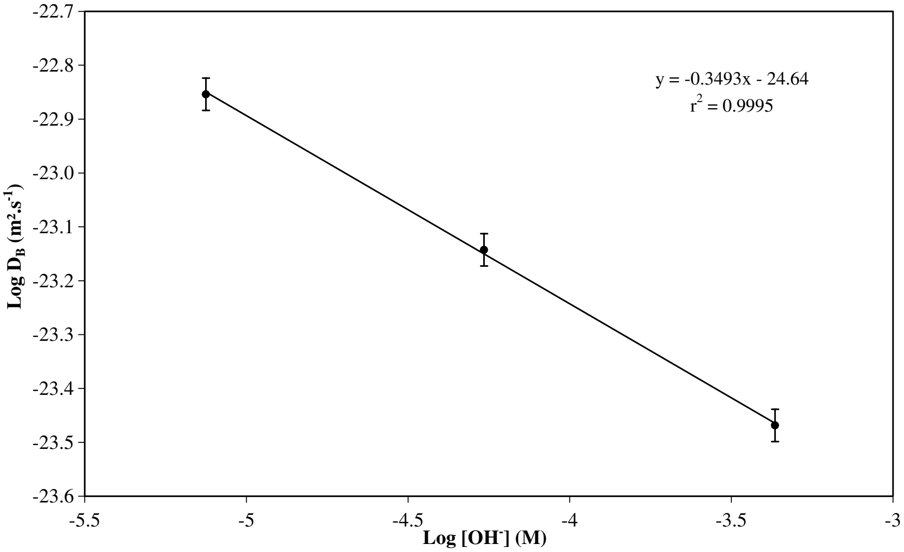

Fig. 3. pH dependency plot for the following experimental conditions: no background electrolytes (initial ionic strength below 5 mM), 323 K, 200 cm^{-1} (experiments 3, 4 and 6). Averaged pH values are converted into hydroxide ion concentration.

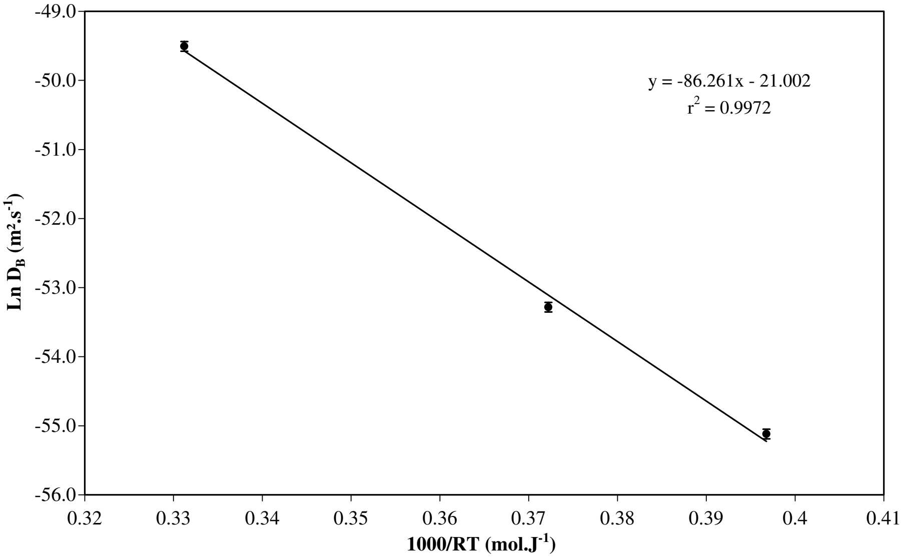

Fig. 4. Temperature dependency plot for the following experimental conditions: no background electrolytes (initial ionic strength below 5 mM), 200 cm^{-1}, 303 K pH 10 ↔ pOH 4.20 (No. 2)/323 K pH 9 ↔ pOH 4.26 (No. 4)/363 K pH8 ↔ pOH 4.04 (No. 9) (pOH values are averaged experimental values).

purpose, pOH is preferred in order to avoid correlation with temperature. This choice is neither established on the diffusion underlying mechanisms nor on the quality of the experimental fits. The study of temperature effect alone is thus simplified by comparing well chosen experiments (Fig. 4) i.e. with the same hydroxide ion concentration.

4.2.1. pH dependency

For the pH dependency at 323 K (Fig. 3), a simple law based on the following equation is used:

$$D = D_0^{\mathrm{pH}}[\mathrm{OH}^-]^{n'}, \tag{6}$$

with $n' = -0.349 \pm 0.03$ and $D_0^{\mathrm{pH}} = 2.29 \times 10^{-25}$ $\mathrm{m}^2\,\mathrm{s}^{-1}$.

As a conclusion, diffusion coefficient decreases by a factor 4 when the pH rises from 8 to 10. This effect is not yet fully understood. One can wonder whether this is due to proton activity and its possibility to exchange with alkali or due to a change in the reactivity of the amorphous interface elements. Bunker and Ernsberger give pieces of information about the interdiffusion mechanisms [18–21]. One assumption is a preferential interaction between the glass network and H_3O^+ ion rather than with HO^- even in basic conditions. Exchanges between alkalis and protons are a common example of such interaction and depend on the surface site acidity. Thus, ion exchange on Si sites can occur below pH 12 and is complete at pH 8 [21]. Even if this reaction does not drastically alter the glass network, since no glass bonds are broken, interdiffusion between water and mobile elements could nevertheless be enhanced when pH decreases from 10 to 8 which is in agreement with the experiments. However, in the case of an exchange between proton and alkali being the limiting mechanism, solutions with high Na^+ and Li^+ concentrations could have been expected to reduce the boron diffusion rate but it was not observed experimentally (Table 2).

This reactive diffusion process, involving water on one hand and glass elements on the other hand, is obviously more complex than a simple exchange reaction since boron, a glass former, presents the same diffusion trend with comparable diffusion coefficient as charge compensator. Indeed, Geneste et al. [17] proved with Ab-Initio calculations that Na^+/H_3O^+ exchange may change the boron coordination since the exchanged protons cannot play the same role as the former sodium charge compensators in the glass. This significant evolution within the glass structure, in presence of water, could explain the almost congruent behaviour of mobile elements whatever their positions in the fresh glass network.

4.2.2. Temperature dependency

In Fig. 4, an Arrhenius behaviour is observed with an activation energy equal to 86.3 kJ mol^{-1} for this diffusion phenomenon. Moreover, if the kinetic rates are plotted instead of the diffusion coefficient for the same experiments, the following value is obtained: 36.7 kJ mol^{-1}. This value is higher than the usual 20 kJ mol^{-1} for pure liquid diffusion and is more suitable for a reactive diffusion where water or protons interact with the material. This result is in good agreement with experimental evidences where glass former like boron are leached as soon as water comes in contact in the same ways as alkalis. Finally, temperature drastically influences on diffusion phenomena around two orders of magnitude on diffusion coefficients between 303 and 363 K.

4.2.3. Diffusion model

pH and temperature were previously considered separately in order to assess each parameter effect on the system. However, both parameters can be coupled in a single equation. For this, former results and current experiments (number 1 and 10 in Table 2) were used to improve the accuracy on diffusion coefficient determination, taking into account both temperature and pH. By considering the equation below (7), E'_a and n' could be fitted with the help of a mathematic solver:

$$D = D_0[\mathrm{OH}^-]^{n'}\mathrm{e}^{-\frac{E'a}{RT}} \tag{7}$$

with $D_0 = 2.21 \times 10^{-11}\,\mathrm{m}^2\,\mathrm{s}^{-1}$, $n' = -0.325$ and $E'_\mathrm{a} = 85.3\mathrm{kJ\,mol}^{-1}$.

This model gives quite good and relevant results with an absolute averaged variance of 14% on diffusion coefficient and 7% on equivalent altered layer thicknesses for a temperature comprised between 303 and 363 K and a pH between 8 and 10 (measured at the experiment temperature).

4.3. Influence of S/V ratio

Looking at the results in Table 2, it appears that there is only a factor 2 between diffusion coefficients in same conditions at two different S/V ratios (e.g. comparison between experiments number 4 and 8

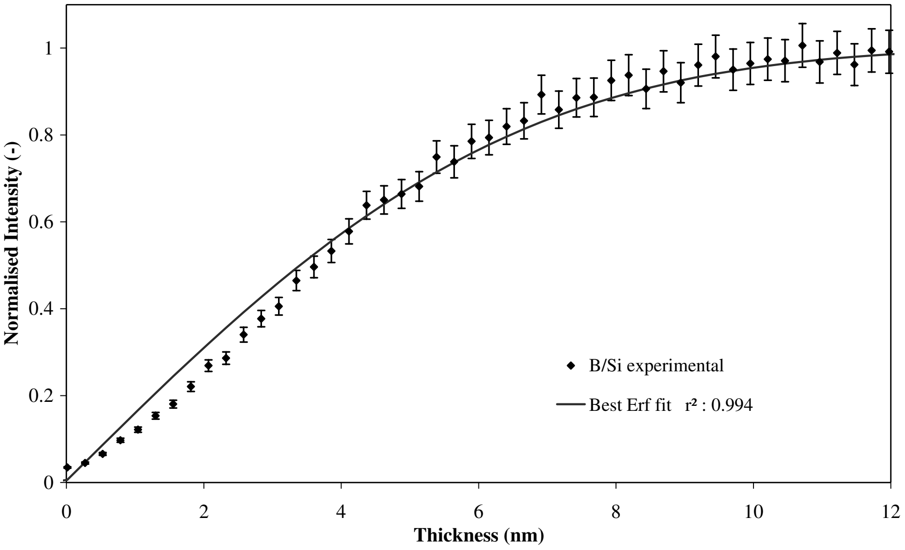

Fig. 5. TOF-SIMS depth profile analysis for the following experimental conditions: 323 K, pH 10, 200 cm^{-1}, no background electrolytes (initial ionic strength below 5 mM). Profile normalised to glass signal. *best erf fit* refers to the closest fit to the experimental data obtained by optimising D value in equation: $\frac{C}{C_0} = \text{erf}\left(\frac{x}{2\sqrt{D \cdot t}}\right)$. Goodness-of-fit is based on lesser square method between experimental data and above equation with determined D value.

or 5 and 7). This is not a drastic effect. It cannot be explained by the ionic strength but rather by a local pH increase. In an experiment at 2000 cm^{-1}, the mass of glass powder is ten times larger than for a 200 cm^{-1} experiment which is equivalent to a 1 cm thick glass powder layer. As the reactor is not always under mechanical agitation, local pH increases are expected within the thick glass layer due to alkali release and could lead to a decrease in diffusion coefficient as previously explained in this paper. Finally, considering S/V ratio, one can notice since diffusion coefficient poorly depends on S/V ratio, that mobile element release is almost proportional to the glass surface all things being equal. Thus, local pH should all the more increase as S/V ratio is high.

4.4. TOF-SIMS comparison

TOF-SIMS results are finally considered. The method is here illustrated with the following experimental conditions: 323 K, 200 cm^{-1}, pH 10. The sample is analysed by TOF-SIMS after 2 months in initially Si saturated solution.

The boron depth profile normalised on silicon profile and glass signal and the best erf fit are shown in Fig. 5. Equivalent diffusion coefficient according to solid depth profile is around $2.2 \times 10^{-24}\ \text{m}^2\ \text{s}^{-1}$ which is in quite good agreement with solution analysis value of $3.2 \times 10^{-24}\ \text{m}^2\ \text{s}^{-1}$.

Nevertheless, changes in diffusion profiles are expected with time due to gel layer evolution [1–6]. This could imply some modifications in solid model approach and assumptions of non-constant diffusion coefficients could be considered for high reaction progress samples. Further studies are therefore needed in order to conclude if this diffusion coefficient determination method is relevant or not for all sample regardless their leaching time. Nevertheless, first tests on early time altered glass are quite satisfying and a detailed study of each element profile is in progress.

5. Conclusion

New evidences are brought for a complex and reactive solid state diffusion of both alkali and boron within glass and its amorphous alteration layer. The influence of parameters such as temperature and pH are investigated and modelled based on boron release. Profile analyses performed at the nanometric scale thanks to TOF-SIMS are consistent with solution analyses. They should bring soon some interesting answers concerning the specific behaviour of alkali, water, and other elements in the alteration process. It should enable to achieve a better understanding of the mechanisms involving diffusion processes: water diffusion, mobile element diffusion or inter diffusion between two entities.

References

[1] S. Gin, P. Frugier, Mater. Res. Soc. Symp. Proc. 807 (2003) 175.

[2] T. Advocat, PhD thesis of the Louis Pasteur University of Strasbourg, France, 1991.

[3] P. Aagaard, H.C. Helgeson, Am. J. Sci. 282 (1982) 237.

[4] B. Grambow, Mater. Res. Soc. Symp. Proc. 44 (1985) 15.

[5] T. Advocat, J.L. Crovisier, B. Fritz, E. Vernaz, Mater. Res. Soc. Symp. Proc. 176 (1990) 241.

[6] D. Rebiscoul, A. Van der Lee, F. Rieutord, F. Né, O. Spalla, A. El-Mansouri, P. Frugier, A. Ayral, S. Gin, J. Nucl. Mater. 326 (2004) 9.

[7] D. Rebiscoul, A. Van der Lee, P. Frugier, A. Ayral, S. Gin, J. Non-Cryst. Solids 325 (2003) 113.

[8] S. Gin, I. Ribet, M. Couillaud, J. Nucl. Mater. 298 (2001) 1.

[9] S. Gin, N. Godon, I. Ribet, P. Jollivet, P. Frugier, Y. Minet, E. Vernaz, J.M. Cavedon, B. Bonin, R. Do Quang, Mater. Res. Soc. Symp. Proc. 824 (2004) 327.

[10] E. Vernaz, J.L. Dussossoy, Appl. Geochem. Suppl. (1) (1992) 13.

[11] J.L. Crovisier, E. Vernaz, J.L. Dussossoy, J. Caurel, Appl. Clay Sci. 7 (2005) 47.

[12] J. Caurel, E. Vernaz, CEA. RT/DRDD/No. 179, 1998, 1–95.

[13] K. Ferrand, PhD thesis of Ecole des Mines of Nantes, France, 2004.

[14] I. Munier, J.-L. Crovisier, B. Grambow, B. Fritz, A. Clement, J. Nucl. Mater. 324 (2004) 97.

[15] J. Crank, Mathematics of Diffusion, second Ed., Oxford University, 1975, ISBN 0198534116 (Chapter 3.3).

[16] A. Ledieu, PhD thesis of Ecole Polytechnique, France, 2005.

[17] G. Geneste, F. Bouhier, S. Gin, J. Non-Cryst. Solids 352 (2006) 3147.

[18] B.C. Bunker, D.R. Tallant, T.J. Headley, G.L. Turner, R.J. Kirkpatrick, Phys. Chem. Glasses 29 (1988) 106.

[19] B.C. Bunker, J. Non-Cryst. Solids 179 (1994) 300.

[20] F.M. Ernsberger, Phys. Chem. Glasses 21 (1980) 146.

[21] B.C. Bunker, Mater. Res. Soc. Symp. Proc. 84 (1987) 493.